Sensors & Actuators: B. Chemical 369 (2022) 132333

Contents lists available at ScienceDirect

Sensors and Actuators: B. Chemical

journal homepage: www.elsevier.com/locate/snb

Photothermal multi-species detection in a hollow-core fiber with frequency-division multiplexing

Zhen Wang [a,b,1], Hui Zhang [a,c,1], Jianing Wang [a], Shoulin Jiang [d], Shoufei Gao [e], Yingying Wang [e], Wei Jin [d], Qiang Wang [a,c,*], Wei Ren [b]

[a] State Key Laboratory of Applied Optics, Changchun Institute of Optics, Fine Mechanics and Physics, Chinese Academy of Sciences, Changchun 130033, China
[b] Department of Mechanical and Automation Engineering, and Shenzhen Research Institute, The Chinese University of Hong Kong, Hong Kong Special Adminitrative region of China
[c] University of Chinese Academy of Sciences, Beijing 100049, China
[d] Department of Electrical Engineering, The Hong Kong Polytechnic University, Kowloon, Hong Kong Special Adminitrative region of China
[e] Institute of Photonics Technology, Jinan University, Guangzhou 510632, China

ARTICLE INFO

Keywords:
Photothermal spectroscopy
Multi-species detection
Frequency-division multiplexing
Hollow-core fiber

ABSTRACT

A photothermal gas sensor has been developed for simultaneous multi-species detection in a hollow-core fiber based on the frequency-division multiplexing technique. By passing multiple pump lasers and a probe laser through a gas-filled hollow-core anti-resonant fiber (HC-ARF), the absorption-generated modulation of the refractive index at various frequencies is sensitively detected by an in-line interferometer. Three distributed-feedback diode lasers at C-band, L-band and U-band are employed as pump lasers for C_2H_2, CO_2 and CH_4 detection. Assisted by optical power amplifiers, the sensor achieves noise equivalent concentrations of 2.5 ppb, 21 ppm and 200 ppb for C_2H_2, CO_2 and CH_4, respectively. The sensor demonstrates excellent linear response to gas concentrations with R-square values between 0.996 and 0.999. Measurement of the three gas species with time-varying concentrations, as well as the aforementioned experiments, further validates the simultaneous multi-species detection with high sensitivity, compact size, and extremely low gas consumption.

1. Introduction

Trace gas detection based on laser absorption spectroscopy (LAS) plays an important role in atmospheric monitoring [1], industrial emissions control [2], energy system [3] and human breath analysis [4] due to its high sensitivity and selectivity. LAS relies on the Beer-Lambert law, which describes the absorption of photons by gas molecules at a resonant frequency [5]. Among different absorption-based techniques, gas sensors based on photoacoustic spectroscopy (PAS) [6,7] and photothermal spectroscopy (PTS) [8–14] have been attracting increasing attention due to the unique advantages of compact size and low cost. The basic principle of PTS is based on the periodic V-T (vibration--translation) relaxation process of gas molecules. The molecules are excited to a vibrational state after absorbing photons and back to the ground state through collisions, converting the photon energy into translational energy of molecules. The periodic process can induce refractive index variation which is detected by an interferometer. Besides, another kind of novel photothermal technique was invented by utilizing the thermoelastic effect of a quartz tuning fork [15–17].

Recent years have witnessed a rapid development of PTS with hollow-core fibers (HCFs), in which the laser intensity is dramatically enhanced attributed to its μm-sized mode field diameter (MFD). In 2015, a hollow-core photonic bandgap fiber (HC-PBF) was first deployed in PTS, where the HC-PBF acted as a gas cell as well to generate strong laser-molecule interaction in an extremely small volume over a long optical path [12]. The photothermal effect can be enhanced by several orders of magnitude, compared with free-space case, showing the potential of ultra-high sensitivity and wide dynamic range. With the advent of mid-infrared HCFs and laser sources such as quantum cascade laser (QCL) and interband cascade laser (ICL), PTS found its applications in mid-infrared region [18,19], where fundamental bands of the many important species are located. This provides larger molecular absorption

* Corresponding author at: State Key Laboratory of Applied Optics, Changchun Institute of Optics, Fine Mechanics and Physics, Chinese Academy of Sciences, Changchun 130033, China.
E-mail address: wangqiang@ciomp.ac.cn (Q. Wang).
[1] These authors contributed equally to this work.

https://doi.org/10.1016/j.snb.2022.132333
Received 12 May 2022; Received in revised form 16 June 2022; Accepted 5 July 2022
Available online 8 July 2022

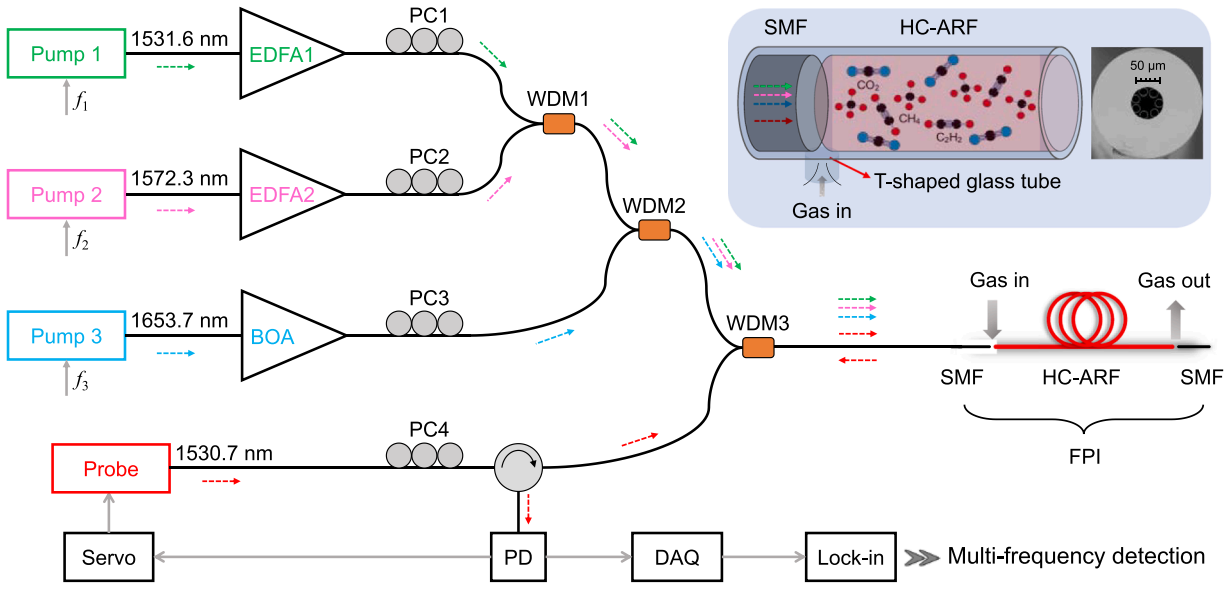

Fig. 1. Schematic of the photothermal multi-species sensor system. EDFA, erbium-doped fiber amplifier; BOA, booster optical amplifier; PC, polarization controller; WDM, wavelength division multiplexing; FPI, Fabry–P é rot interferometer; SMF, single mode fibers; PD, photodetector; DAQ, data acquisition card. Inset: scanning electron microscope (SEM) image of the cross-section of the hollow-core anti-resonant fiber (HC-ARF), and the schematic of the HC-ARF FPI.

cross sections by one to three orders compared to those in the near-infrared region. Besides, different intriguing optical techniques were also introduced to boost the sensitivity of PTS to parts-per-billion (ppb) even parts-per-trillion (ppt) levels, such as pump laser power enhancement by PTS implementation inside a fiber-ring laser cavity [20], phase modulation amplification by locking the probe and pump lasers to an HCF-based Fabry–P é rot cavity [21], and external perturbation phase noise minimization by developing transverse mode interference spectrometer [14].

To date, most works were performed with a single frequency laser targeting only one species. However, the detection of multi-species is practically demanded for a sensor in many specific applications. For example, in human breath analysis, some volatile organic compounds (VOCs) and carbon isotopes have been established as biomarkers, whose concentrations would collectively aid in disease diagnosis [4]. In industrial emissions control, the gas denitrification process in power plants critically relies on the measurement of water vapor, nitrogen oxides (NO_x) and NH_3 [22]. Simultaneous detection of ocean dissolved gases like CO_2, O_2, and H_2 provides important information for the study of marine ecology, in which only a limited amount of dissolved gas analyte can be used for analysis [23]. In environmental monitoring, the transport, sources, and sinks of greenhouse gases (CH_4, CO_2, etc.) require accurate and continuous measurements at a low cost [24]. Recently, the feasibility of PTS for multi-species detection was demonstrated using time-division multiplexing [25]. Different species must be separately interrogated in a time-consuming order due to the existing time gap between each measurement. Hence, the simultaneous measurement of multi-species remains a challenge to be solved especially for scenarios, where only a limited sample amount can be expected or the variation tendency of relevant species needs to be investigated.

In this work, a gas sensor with an all-fiber configuration based on PTS and frequency-division multiplexing (FDM) is proposed for simultaneous multi-species detection. The μm-sized diameter of the HCF with a short length provides sub-microliter gas consumption. As an example, three diode lasers with center wavelengths located at C-band, L-band and U-band are integrated to interrogate C_2H_2, CO_2, and CH_4, respectively. The performance of the sensor including the detection limit, linear response, simultaneous measurement, and long-term stability is experimentally investigated in detail.

2. Frequency-division multiplexing in photothermal spectroscopy

A pump-probe configuration is often adopted for PTS. When the wavelength-modulated pump laser is in resonance with the gas molecules, the absorption-induced phase modulation is detected by a probe-laser-based interferometer. As introduced previously, an HCF provides a significantly increased light intensity and highly efficient light-molecule interaction within the μm-sized hollow core. To achieve multi-species detection using FDM, the wavelength of each pump laser is modulated at different frequencies. The induced phase modulation by pump lasers along the HCF can be expressed by [12].

$$\Delta\phi \propto k^* \cdot L \cdot \left\{ A \cdot \overline{\chi}(\lambda[f]) \cdot \overline{P}_{pump} \right\}_n \tag{1}$$

where the subscripter n (1, 2, 3, etc.) is the index of pump lasers, k^* is a coefficient inversely proportional to the cross area of the MFD, L is the fiber length, A is the peak absorption coefficient, $\overline{\chi}(\lambda[f])$ is the normalized line-shape function of the absorption feature, $\lambda[f]$ is the laser wavelength that is modulated at frequency f, $\overline{P}_{pump}$ is the average laser power over the whole hollow core fiber, for a thin absorption, i.e., $A \cdot L \ll 1$. Deriving from the line-shape function of the absorption feature, the harmonics (1 f, 2 f, 3 f, etc.) of phase modulation exist and can be simultaneously detected by an interferometer.

We use an in-line Fabry–P é rot interferometer (FPI) with a probe laser for phase modulation detection. The FPI is formed by natural reflections at the joints between the HCF and single mode fibers (SMFs) [26]. In this case, the photothermal-induced refractive index modulation is encoded in the phase of the probe laser. The probe light exits from the input of the FPI, which carries the photothermal information, will interfere with the directly reflected one with no phase modulation. Two reflection beams and the interference process can be expressed by the following time-domain form of electrical fields

$$E_1 = A_1 cos(\omega t + \varphi_0) \tag{2}$$

$$E_2 = A_2 cos(\omega t + \varphi_0 + 2 \cdot \Delta\varphi) \tag{3}$$

$$(E_1 + E_2)^2 = E_1^2 + E_2^2 + A_1 A_2 cos(2 \cdot \Delta\varphi) \tag{4}$$

where A_1 and A_2 are amplitudes, ω is the angular frequency of the probe

Table 1
The selected absorption lines and corresponding line intensities of C_2H_2, CO_2, and CH_4.

Molecule	Wavenumber (cm^{-1})	Line intensity (cm^{-1}·(mol·cm^{-2})$^{-1}$)
C_2H_2	6529.17	1.165×10^{-20}
CO_2	6359.97	1.761×10^{-23}
CH_4	6046.96	1.455×10^{-21}

laser, φ_0 is the initial phase of the probe laser, $\Delta\varphi$ is phase modulation induced by the photothermal effect in which the factor 2 accounts for the single round trip of the probe laser in the FPI. Based on Eqs. (1) and (4), harmonics of phase modulation corresponding to different fundamental frequencies of wavelength modulation can be demodulated simultaneously by a lock-in amplifier. Note that a hollow-core anti-resonant fiber (HC-ARF) is utilized in this work instead of the commercially available HC-PBF. Compared with HC-PBF, the HC-ARF usually exhibits a relatively larger air core to facilitate the gas loading and much lower mode interference noise because the guided fundamental mode is kept away from silica junctions where cladding modes are significant [27].

3. Experimental apparatus

The experimental setup of the sensor is shown in Fig. 1. The core sensing part is the FPI, formed by the HC-ARF and SMFs. The HC-ARF with a length of 7 cm and an air-core diameter of 28 μm acts as a gas cell, providing a gas consumption of only 0.17 μL. The gas samples are pressurized into the HC-ARF microchannels from a small gap (about 2 μm) at the HC-ARF/SMF joints. Three diode lasers with wavelengths of 1531.6 nm, 1572.3 nm and 1653.7 nm are used as pump lasers to interrogate C_2H_2, CO_2 and CH_4, respectively. The selected absorption lines and the corresponding line intensities from HITRAN database are listed in Table 1 [28]. We employ two erbium-doped fiber amplifiers (EDFAs) and one booster optical amplifier (BOA) to amplify the pump powers. Three polarization controllers (PC) are used to optimize the polarization of three pump lasers to maximize the corresponding effective pump power inside the HC-ARF.

For multi-species detection, three pump lasers and one probe laser are combined and delivered into the FPI simultaneously via three WDMs. The WDM1 in Fig. 1 has two narrow input channels for 1531.6 nm and 1572.3 nm. The combination of two lasers is delivered into the broadband input channel of WDM2 and the other narrow channel is designed for 1653.7 nm. Finally, the WDM3 combines the three pump lasers and the probe laser. The pump powers for C_2H_2, CO_2 and CH_4 detection are 240 mW, 62 mW and 57 mW, respectively. The input channel of the WDM3 for probe laser has a center wavelength of 1530.7 nm, which is chosen away from any gas absorption, and a narrow bandwidth of 200 GHz, which can sufficiently filter the cross-talk pump laser reflected by the FPI.

Three current modulation frequencies of 23 kHz, 3 kHz and 8.5 kHz are applied on the pump lasers for C_2H_2, CO_2 and CH_4 detection, respectively. The modulation frequencies are selected considering the response bandwidth of the FPI and the different relaxation rates of the three gas molecules. The wavelength modulations of the pump lasers can generate refractive index modulation inside the HC-ARF which can be detected by the probe-laser-based interferometer. The probe laser works at the quadrature point of the interferometer, corresponding to the maximum frequency-to-intensity conversion efficiency. Another PC is used to control the probe laser polarization to optimize the contrast of interference fringes. The refractive index modulations at various frequencies are encoded into the phase of the probe laser, which is converted into the corresponding intensity modulation and detected by one single photodetector. The low-frequency part is used to stabilize the probe laser. The high-frequency part is demodulated in the second harmonic regime ($2f$) by one lock-in amplifier, which comprises three separate demodulators sharing the same input channel.

4. Results and discussion

4.1. Modulation depth optimization

The PTS signal is related to the modulation depth which needs to be optimized to obtain the largest $2f$ amplitude. The amplitude of PTS signal for a mixture of 1000 ppm C_2H_2/N_2, 10 % CO_2/N_2 and 1 % CH_4/N_2 are experimentally investigated at varied modulation current for this purpose. As shown in Fig. 2, the amplitude of PTS signal increases with the modulation depth first and then reaches a plateau. We adopt 12.5 mA, 15 mA and 10 mA as the optimum modulation depths for C_2H_2, CO_2 and CH_4 respectively for the following experiments. All the amplitudes in Fig. 2 are normalized just for viewing purposes.

4.2. Photothermal spectroscopy measurement

To evaluate the sensor performance, gas mixtures of known concentrations are generated by diluting 1000 ppm C_2H_2/N_2, pure CO_2 and 1 % CH_4/N_2 by pure N_2 using a commercial gas dilution instrument. Three different kinds of gas mixtures are introduced into the sensor individually. Fig. 3 depicts the representative PTS-$2f$ signal of the three gas species at different gas concentrations which are measured at 760 torr. The linear responses of the sensor to the three gas species are separately investigated by measuring the corresponding amplitudes of the PTS signal and plotted in Fig. 4 as a function of gas concentration. The concentration ranges are 1–1000 ppm for C_2H_2/N_2, 1–10 % for CO_2/N_2 and 100–10000 ppm for CH_4/N_2. The linear fit to the experimental data yields R-square values of 0.996, 0.999, 0.999 and linear slope of 1.23 μV/ppm, 1.70 μV/1 %, 0.02 μV/ppm, for C_2H_2/N_2, CO_2/N_2 and CH_4/N_2, respectively.

The capability of simultaneous measurement is validated by detecting the three gas species in the HC-ARF. We program the gas dilution instrument to generate gas samples with time-varying concentrations

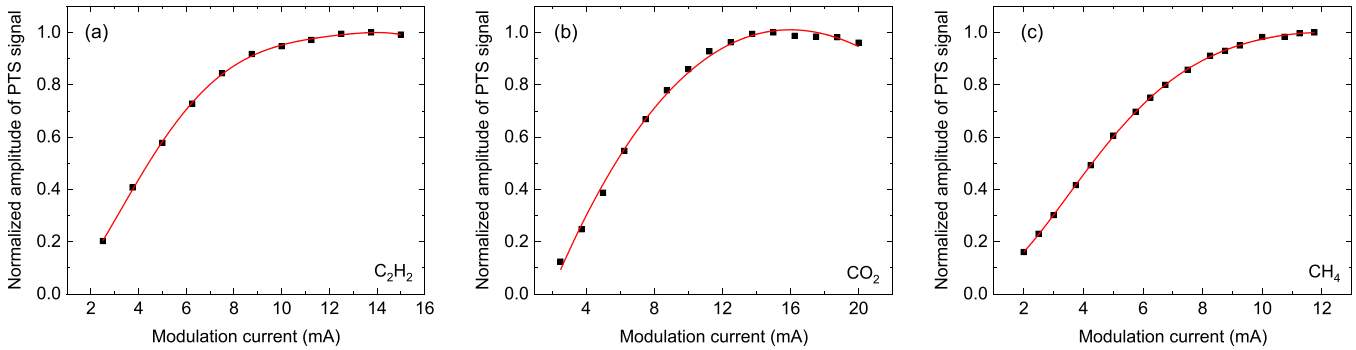

Fig. 2. Measured amplitudes of PTS signal of (a) C_2H_2, (b) CO_2 and (c) CH_4 as a function of laser modulation depth.

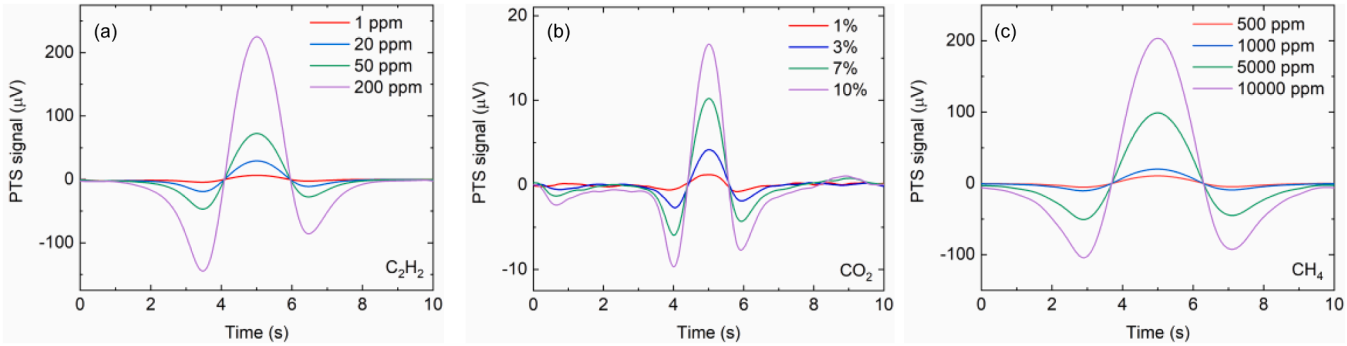

Fig. 3. Representative PTS signals recorded with different concentrations of (a) C_2H_2, (b) CO_2 and (c) CH_4 at 760 torr.

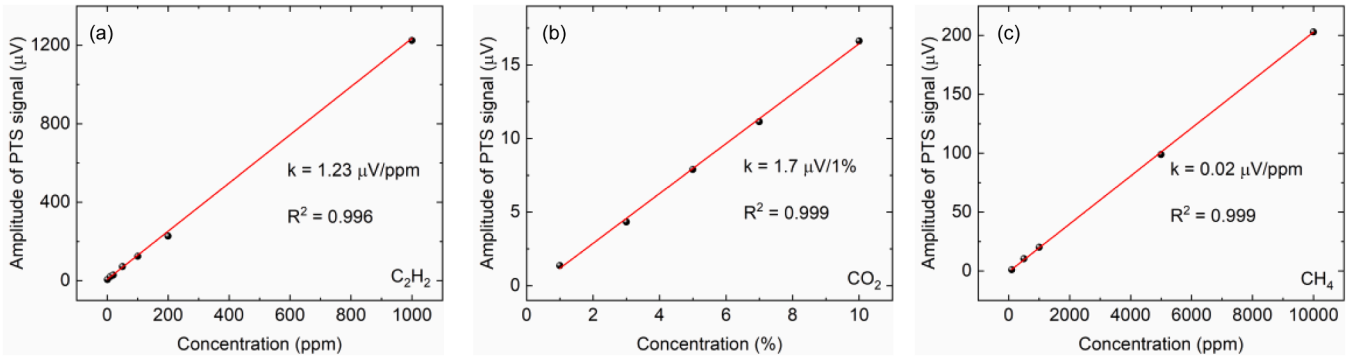

Fig. 4. Linearity of the amplitude of PTS signal to concentrations of (a) C_2H_2, (b) CO_2 and (c) CH_4.

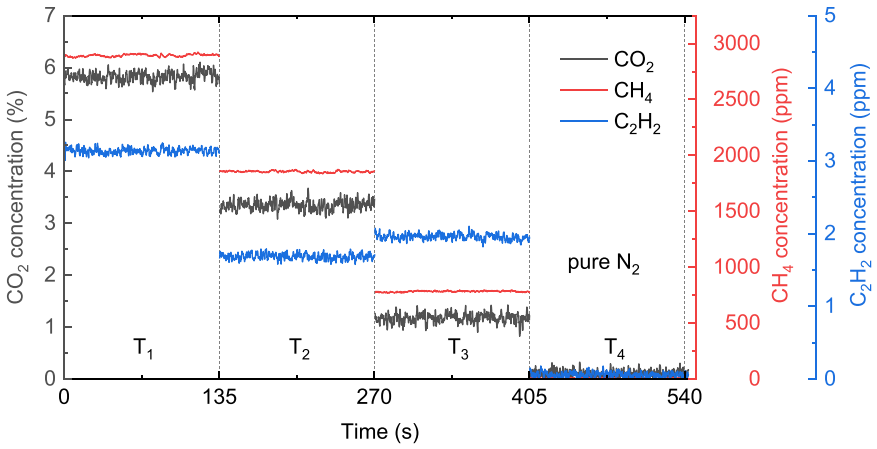

Fig. 5. Simultaneous detection of the three species with varying concentrations in four successive cases. Each laser wavelength is tuned to the peak of the corresponding absorption line. The gas samples are generated by diluting the three calibrated gas species simultaneously.

and the measurement of each case (T_1, T_2, T_3, T_4 in Fig. 5) lasts for about 135 s. In this test, the wavelengths of the three pump lasers are tuned to the absorption peaks of the corresponding molecules. Fig. 5 depicts the response curves of the sensor to different mixtures of the three gas species in four successive cases, which match well with the pre-set conditions.

4.3. Detection limit

To further evaluate the sensitivity and stability of the sensor, we perform Allan deviation analysis by measuring pure N_2 for about one hour at a pressure of 760 torr with the results illustrated in Fig. 6. The three plots correspond to different detection frequencies of the three wavelengths. According to Fig. 6(a), the sensor achieves a sensitivity of 21 ppb for C_2H_2 detection at an integration time of 1 s. The turning point of the curve at about 200 s leads to a minimum detection limit (MDL) of ~2.5 ppb, corresponding to a normalized noise equivalent absorption (NNEA) coefficient of 1×10^{-8} $cm^{-1}{\cdot}W/Hz^{1/2}$. Considering the maximum concentration of 1000 ppm in the linear curve, the dynamic range is beyond 4 orders of magnitude for C_2H_2 detection. Similarly, the Allan deviation curves corresponding to CO_2 and CH_4 in Fig. 6(b) and (c) show that the sensor achieves an MDL of 21 ppm for CO_2 and 200 ppb for CH_4 detection at an integration time of 400 s and 200 s, respectively. Table 2 summaries the MDL, NNEA, and dynamic range of the sensor for the gas species. One limitation factor for the sensitivity is the interference fringes of pump lasers in the interferometer. The issue can be solved by adding a dielectric coating on the facets of SMFs. The coating should have a high reflectivity for the probe laser to enhance the effective

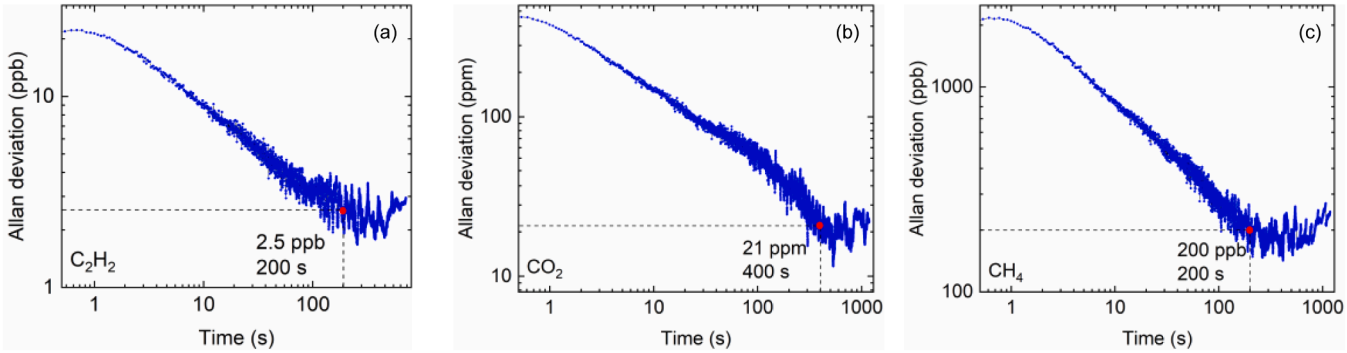

Fig. 6. Allan deviation plots of noise at 760 torr for the detection of (a) C_2H_2, (b) CO_2 and (c) CH_4.

Table 2
Summary of the sensor performance including the minimum detection limit (MDL), dynamic range and normalized noise equivalent absorption (NNEA) coefficient for the three gas species.

Wavenumber (cm^{-1})	Gas	MDL	Integration time	Dynamic range	NNEA (cm^{-1}·W/$Hz^{1/2}$)
6529.17	C_2H_2	2.5 ppb	200 s	4×10^5	1×10^{-8}
6359.97	CO_2	21 ppm	400 s	4.8×10^3	4.7×10^{-8}
6046.96	CH_4	200 ppb	200 s	5×10^4	6×10^{-8}

interference and high transmissivity for pump to reduce the interference fringes.

5. Conclusions

We have demonstrated a trace gas sensor based on PTS and FDM for the simultaneous detection of multi-species. Within an all-fiber structure, three pump lasers and one probe laser are confined in an HC-ARF, which also acts as a gas cell and an interferometer at the same time. The linear response and the ability of simultaneous detection of the multi-species have been demonstrated. The sensor achieves minimum detection limits of 2.5 ppb, 21 ppm and 200 ppb for C_2H_2, CO_2 and CH_4, respectively. With the high sensitivity, low gas consumption, compact and flexible structure, the developed gas sensor is promising in many field applications. Future work will involve the improvement of the detection sensitivity by employing longer hollow-core fiber and mid-infrared pump lasers which covers the fundamental bands of gas molecules.

CRediT authorship contribution statement

Zhen Wang: Conceptualization, Methodology, Investigation, Writing – original draft. **Hui Zhang**: Data curation, Validation, Writing – original draft. **Jianing Wang**: Resources, Writing – review & editing. **Shoulin Jiang**: Resources, Investigation. **Shoufei Gao**: Methodology, Formal analysis. **Yingying Wang**: Resources, Methodology. **Wei Jin**: Resources, Methodology. **Qiang Wang**: Conceptualization, Methodology, Writing – review & editing, Supervision, Project administration, Funding acquisition. **Wei Ren**: Resources, Supervision, Writing – review & editing, Funding acquisition.

Declaration of Competing Interest

The authors declare that they have no known competing financial interests or personal relationships that could have appeared to influence the work reported in this paper.

Acknowledgements

This research was supported by the Second Comprehensive Scientific Investigation of the Qinghai-Tibet Plateau (2019QZKK020802), National Natural Science Foundation of China (NSFC) (62005267, 62005268), Scientific Instrument Developing Project of the Chinese Academy of Sciences (YJKYYQ20190037), Strategic Priority Research Program of Chinese Academy of Sciences (XDA17040513, XDA22020502), and Young Talent of Lifting Engineering for Science and Technology in Jilin, China (QT202106).

References

[1] H. Wu, L. Dong, X. Yin, A. Sampaolo, P. Patimisco, W. Ma, L. Zhang, W. Yin, L. Xiao, V. Spagnolo, S. Jia, Atmospheric CH_4 measurement near a landfill using an ICL-based QEPAS sensor with VT relaxation self-calibration, Sens. Actuators B Chem. 297 (2019), 126753.
[2] C. Shi, D. Wang, Z. Wang, L. Ma, Q. Wang, K. Xu, S. Chen, W. Ren, A mid-infrared fiber-coupled QEPAS nitric oxide sensor for real-time engine exhaust monitoring, IEEE Sens. J. 17 (2017) 7418–7424.
[3] A. Farooq, A.B.S. Alquaity, M. Raza, E.F. Nasir, S. Yao, W. Ren, Laser sensors for energy systems and process industries: perspectives and directions, Prog. Energ. Combust. 91 (2022), 100997.
[4] Q. Liang, Y.C. Chan, P.B. Changala, D.J. Nesbitt, J. Ye, J. Toscano, Ultra-sensitive multi-species spectroscopic breath analysis for real-time health monitoring and diagnostics, Proc. Natl. Acad. Sci. U. S. A. 118 (2021), e2105063118.
[5] R.K. Hanson, R.M. Spearrin, C.S. Goldenstein, Spectroscopy and Optical Diagnostics for Gases, Springer, 2016.
[6] H. Wu, L. Dong, H. Zheng, Y. Yu, W. Ma, L. Zhang, W. Yin, L. Xiao, S. Jia, F. K. Tittel, Beat frequency quartz-enhanced photoacoustic spectroscopy for fast and calibration-free continuous trace-gas monitoring, Nat. Commun. 8 (2017) 15331.
[7] P. Patimisco, A. Sampaolo, L. Dong, F.K. Tittel, V. Spagnolo, Recent advances in quartz enhanced photoacoustic sensing, Appl. Phys. Rev. 5 (2018), 011106.
[8] P. Hess, Principles of Photoacoustic and Photothermal Analysis, in: P. Hess (Ed.), Photoacoust. Photothermal Photochem. Process. Gases, Springer, Berlin, Heidelberg, 1989, pp. 1–13.
[9] K. Krzempek, A Review of photothermal detection techniques for gas sensing applications, Appl. Sci. 9 (2019) 2826.
[10] C. Yao, Q. Wang, Y. Lin, W. Jin, L. Xiao, S. Gao, Y. Wang, P. Wang, W. Ren, Photothermal CO detection in a hollow-core negative curvature fiber, Opt. Lett. 44 (2019) 4048–4051.
[11] Q. Wang, Z. Wang, H. Zhang, S. Jiang, Y. Wang, W. Jin, W. Ren, Dual-comb photothermal spectroscopy, Nat. Commun. 13 (2022) 2181.
[12] W. Jin, Y. Cao, F. Yang, H.L. Ho, Ultra-sensitive all-fibre photothermal spectroscopy with large dynamic range, Nat. Commun. 6 (2015) 6767.
[13] J.P. Waclawek, C. Kristament, H. Moser, B. Lendl, Balanced-detection interferometric cavity-assisted photothermal spectroscopy, Opt. Express 27 (2019) 12183–12195.
[14] P. Zhao, Y. Zhao, H. Bao, H.L. Ho, W. Jin, S. Fan, S. Gao, Y. Wang, P. Wang, Mode-phase-difference photothermal spectroscopy for gas detection with an anti-resonant hollow-core optical fiber, Nat. Commun. 11 (2020) 847.
[15] Y. Ma, Y. He, Y. Tong, X. Yu, F.K. Tittel, Quartz-tuning-fork enhanced photothermal spectroscopy for ultra-high sensitive trace gas detection, Opt. Express 26 (2018) 32103–32110.
[16] Y. Ma, W. Feng, S. Qiao, Z. Zhao, S. Gao, Y. Wang, Hollow-core anti-resonant fiber based light-induced thermoelastic spectroscopy for gas sensing, Opt. Express 30 (2022) 18836–18844.
[17] T. Wei, A. Zifarelli, S.D. Russo, H. Wu, G. Menduni, P. Patimisco, A. Sampaolo, V. Spagnolo, L. Dong, High and flat spectral responsivity of quartz tuning fork used as infrared photodetector in tunable diode laser spectroscopy, Appl. Phys. Rev. 8 (2021), 041409.

[18] Z. Li, Z. Wang, F. Yang, W. Jin, W. Ren, Mid-infrared fiber-optic photothermal interferometry, Opt. Lett. 42 (2017) 3718–3721.
[19] C. Yao, S. Gao, Y. Wang, W. Jin, W. Ren, Heterodyne interferometric photothermal spectroscopy for gas detection in a hollow-core fiber, Sens. Actuators B: Chem. 346 (2021), 130528.
[20] Y. Zhao, W. Jin, Y. Lin, F. Yang, H.L. Ho, All-fiber gas sensor with intracavity photothermal spectroscopy, Opt. Lett. 43 (2018) 1566–1569.
[21] H. Bao, W. Jin, Y. Hong, H.L. Ho, S. Gao, Y. Wang, Phase-modulation-amplifying hollow-core fiber photothermal interferometry for ultrasensitive gas sensing, J. Light. Technol. 40 (2022) 313–322.
[22] J. Li, C. Zhang, Y. Wei, Z. Du, F. Sun, Y. Ji, X. Yang, C. Liu, *In situ*, portable and robust laser sensor for simultaneous measurement of ammonia, water vapor and temperature in denitrification processes of coal fired power plants, Sens. Actuators B: Chem. 305 (2020), 127533.
[23] M. Li, Q. Liu, D. Yang, J. Guo, G. Si, L. Wu, R. Zheng, Underwater in situ dissolved gas detection based on multi-reflection Raman spectroscopy, Sensors 21 (2021) 4831.
[24] G.B. Rieker, F.R. Giorgetta, W.C. Swann, J. Kofler, A.M. Zolot, L.C. Sinclair, E. Baumann, C. Cromer, G. Petron, C. Sweeney, P.P. Tans, I. Coddington, N. R. Newbury, Frequency-comb-based remote sensing of greenhouse gases over kilometer air paths, Optica 1 (2014) 290–298.
[25] F. Liu, H. Bao, H.L. Ho, W. Jin, S. Gao, Y. Wang, Multicomponent trace gas detection with hollow-core fiber photothermal interferometry and time-division multiplexing, Opt. Express 29 (2021) 43445–43453.
[26] F. Yang, Y. Tan, W. Jin, Y. Lin, Y. Qi, H.L. Ho, Hollow-core fiber Fabry–Perot photothermal gas sensor, Opt. Lett. 41 (2016) 3025–3028.
[27] C. Yao, L. Xiao, S. Gao, Y. Wang, P. Wang, R. Kan, W. Jin, W. Ren, Sub-ppm CO detection in a sub-meter-long hollow-core negative curvature fiber using absorption spectroscopy at 2.3 μm, Sens. Actuators B: Chem. 303 (2020), 127238.
[28] I.E. Gordon, L.S. Rothman, C. Hill, R.V. Kochanov, Y. Tan, P.F. Bernath, M. Birk, V. Boudon, A. Campargue, K.V. Chance, B.J. Drouin, J.-M. Flaud, R.R. Gamache, J. T. Hodges, D. Jacquemart, V.I. Perevalov, A. Perrin, K.P. Shine, M.-A.H. Smith, J. Tennyson, G.C. Toon, H. Tran, V.G. Tyuterev, A. Barbe, A.G. Császár, V.M. Devi, T. Furtenbacher, J.J. Harrison, J.-M. Hartmann, A. Jolly, T.J. Johnson, T. Karman, I. Kleiner, A.A. Kyuberis, J. Loos, O.M. Lyulin, S.T. Massie, S.N. Mikhailenko, N. Moazzen-Ahmadi, H.S.P. Müller, O.V. Naumenko, A.V. Nikitin, O.L. Polyansky, M. Rey, M. Rotger, S.W. Sharpe, K. Sung, E. Starikova, S.A. Tashkun, J.V. Auwera, G. Wagner, J. Wilzewski, P. Wcisło, S. Yu, E.J. Zak, The HITRAN2016 molecular spectroscopic database, J. Quant. Spectrosc. Radiat. Transf. 203 (2017) 3–69.

Zhen Wang is currently a visiting scholar at Changchun Institute of Optics, Fine Mechanics and Physics, Chinese Academy of Sciences and a postdoc fellow at the National Institute of Optics (CNR-INO) in Italy. His research project is trace gas sensing and laser spectroscopy.

Hui Zhang received his BEng degree from Ocean University of China in 2019. He is currently a PhD student at Changchun Institute of Optics, Fine Mechanics and Physics, Chinese Academy of Sciences. His research project is on fiber sensing and laser spectroscopy.

Jianing Wang received his BEng degree in Photoelectric Information Engineering from Changchun University of Science and Technology in 2010, MSc degree in Electrical and Electronics from and Melbourne University in 2014, and PhD degree in Circuit and System from Jilin University in 2017. He currently works as an assistant professor in Changchun Institute of Optics, Fine Mechanics and Physics (CIOMP). His research interests are infrared absorption spectroscopy, signal processing based on PFGA and optical gas sensors.

Shoulin Jiang received his BEng degree from Xi'an Jiao Tong University in 2014 and Ph. D degree from Shanghai Jiao Tong University in 2019. He studied in the University of Southampton as a visiting student from Oct. 2017 to Sep. 2018. He joined the Shenzhen Research Institution of the Hong Kong Polytechnic University as a postdoc researcher in 2019 and currently works here as an associate research fellow. His research interests include specialty optical fibers, optical devices, and optical gas detectors.

Shoufei Gao received his M.S. and Ph.D. degree in optical engineering from the Beijing University of Technology. Afterwards, he worked as a postdoctoral fellow at the department of Electrical Engineering, The Hong Kong Polytechnic University. He is currently an associate research fellow at Jinan University, China. His research focuses on the new forms of optical fibers and their applications.

Yingying Wang is currently the professor at Jinan University, China. She obtained her Ph. D. degree from the University of Bath in 2011. From 2010–2012, she worked as a postdoctoral fellow at the University of Bath and the University of Limoges, respectively. From 2012–2019, she worked at Beijing University of Technology. Her main research fields are photonic crystal fibers and their applications.

Wei Jin received his BEng and MSc degrees from Beijing University of Aeronautics and Astronautics in 1984 and 1987, respectively. He received the Ph.D. degree in 1991 in fiber optics from University of Strathclyde and afterwards was employed as a Postdoctoral Research Fellow at the same University till the end of 1995. He joined the Department of Electrical Engineering of the Hong Kong Polytechnic University as an assistant Professor in 1996 and was promoted to an associate professor in 1998 and a professor in 2003. His research interests are photonic crystal fibers and devices, optical fiber sensors, fiber lasers and amplifiers, and optical gas detectors. Prof. Jin is a fellow of OSA, a senior member of IEEE, a member of SPIE.

Qiang Wang is currently a professor in the State Key Laboratory of Applied Optics at Changchun Institute of Optics, Fine Mechanics and Physics, Chinese Academy of Sciences. He received his B.S. degree in Electronic Science and Technology in 2011 and Ph.D. degree in Optical Engineering in 2016 from Shandong University. After his graduate study, he worked as a postdoctoral fellow at the Chinese University of Hong Kong and Max Planck Institute of Quantum Optics successively. His recent research interests are laser spectroscopy, optical sensing, and engineering application of trace gas analysis in the atmosphere, deep sea, and public health.

Wei Ren received the B.S. degree in Mechanical Engineering and M.S. degree in Optical Engineering from Tsinghua University in 2006 and 2008, respectively. He received the Ph. D. degree in Mechanical Engineering from Stanford University in 2013. He was awarded the Robert A. Welch Foundation postdoctoral fellowship to work in the Department of Electrical and Computer Engineering at Rice University in 2013–14. Dr. Ren is now an associate professor in the Department of Mechanical and Automation Engineering at the Chinese University of Hong Kong. His research to date has resulted in more than 70 peer-reviewed journal publications in laser spectroscopy, optical sensing, and chemical kinetics. He is currently the co-editor of Springer journal Applied Physics B. Prof. Ren is the senior member of OSA, and member of SPIE and the Combustion Institute.